THE JOURNAL OF PHYSICAL CHEMISTRY B

pubs.acs.org/JPCB Article

The Role of the Solvent in the Condensed-Phase Dynamics and Identity of Chemical Bonds: The Case of the Sodium Dimer Cation in THF

Published as part of The Journal of Physical Chemistry virtual special issue "Peter J. Rossky Festschrift".

Devon R. Widmer and Benjamin J. Schwartz*

Cite This: *J. Phys. Chem. B* 2020, 124, 6603–6616 Read Online

ACCESS | Metrics & More | Article Recommendations | Supporting Information

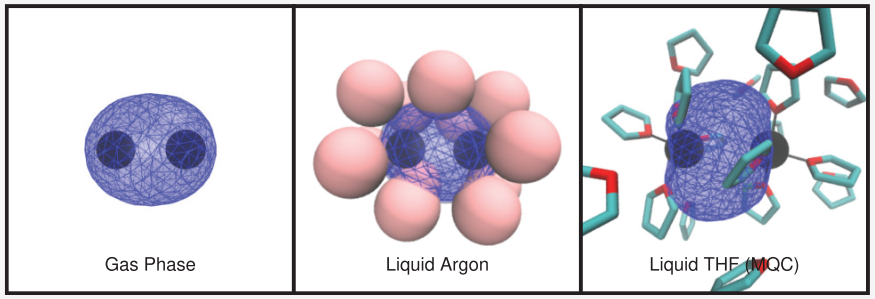

ABSTRACT: When a solute molecule is placed in solution, is it acceptable to presume that its electronic structure is essentially the same as that in the gas phase? In this paper, we address this question from a simulation perspective for the case of the sodium dimer cation (Na_2^+) molecule in both liquid Ar and liquid tetrahydrofuran (THF). In previous work, we showed that, when local specific interactions between a solute and solvent are energetically on the order of a hydrogen bond, the solvent can become part of the chemical identity of the solute. Here, using mixed quantum/classical molecular dynamics simulations, we see that, for the Na_2^+ molecule, solute–solvent interactions lead to two stable, chemically distinct coordination states ($Na(THF)_4$–$Na(THF)_5^+$ and $Na(THF)_5$–$Na(THF)_5^+$) that are not only stable themselves as gas-phase molecules but that also have a completely new electronic structure with important implications for the excited-state photodissociation of this molecule in the condensed phase. Furthermore, we show through a set of comparative classical simulations that treating the solute's bonding electron explicitly quantum mechanically is necessary to understand both the ground-state dynamics and chemical identity of this simple diatomic molecule; even use of the quantum-derived potential of mean force is insufficient to describe the behavior of the molecule classically. Finally, we calculate the results of a proposed transient hole-burning experiment that could be used to spectroscopically disentangle the presence of the different coordination states.

Downloaded via UNIV OF CALIFORNIA LOS ANGELES on October 11, 2020 at 06:31:44 (UTC).
See https://pubs.acs.org/sharingguidelines for options on how to legitimately share published articles.

INTRODUCTION

Solvent molecules, although usually assumed to be mere spectators in condensed-phase chemical reactions, not only can dictate a solute's bond dynamics, thus playing a key role in the solute's reactivity, but are also capable of helping to form new chemical species that are distinct both in behavior and reactivity compared to the original solute.[1] The effects of solvent interactions on the electronic structure of solutes go beyond well-studied cases where the solvent is known to create the solute's electronic structure, such as for solvated electrons[2] or the charge-transfer-to-solvent transitions of simple anions.[3] For example, in electron transfer reactions, the reorganization of the solvent is usually the driving force that moves the electron from donor to acceptor.[4−6] And in photodissociation reactions, the "cage" of solvent molecules that surrounds any given solute prevents the breaking of chemical bonds by trapping the geminate photofragment pair. This forces the bond to reform if the fragments are unable to escape the solvent cage.[7] In previous work, our group showed that the solvent can affect chemical bonds in yet another way: Pauli repulsion interactions from the surrounding solvent can compress a solute's bonding electrons, decreasing the bond length, increasing the bond vibrational frequency, blue-shifting the electronic absorption, and inducing relatively large instantaneous dipole moments, even without electrostatic forces.[8]

Received: April 13, 2020
Revised: June 30, 2020
Published: June 30, 2020

ACS Publications © 2020 American Chemical Society

https://dx.doi.org/10.1021/acs.jpcb.0c03298
J. Phys. Chem. B 2020, 124, 6603–6616

Beyond these general solute−solvent interactions, when there are local specific interactions between a solute and solvent that are energetically on the order of that of a hydrogen bond, an entirely new chemical effect can occur: solvent molecules can incorporate themselves as an integral part of the solute's chemical identity. We identified an example of this phenomenon in a previous study of the sodium dimer (Na_2) in liquid tetrahydrofuran (THF).[1] We found that dative bonds formed between the sodium cation cores within the molecule and the lone pairs on the THF oxygen atoms. These interactions produced three discrete new solutes, $Na(THF)_2$−$Na(THF)_4$, $Na(THF)_3$−$Na(THF)_3$, and $Na(THF)_3$−$Na(THF)_4$, due to different degrees of solvent coordination. These stable coordination states interconverted by overcoming an energy barrier of ∼8 k_BT. In other words, the equilibrium involving breaking and/or formation of a Na^+−THF dative bond constitutes a chemical reaction that converts one unique chemical species into another.[1]

In this work, we have chosen to further explore how solvents with modest local specific interactions influence the electronic structure and chemical identity of solutes by studying the Na_2^+ molecule. We make this choice for several reasons. First, Na_2^+ has a relatively simple electronic structure that can be well described in mixed quantum/classical (MQC) molecular dynamics (MD) simulations. This provides an excellent point of comparison to our previous work on the behavior of the solvated Na_2 molecule,[1] allowing us to explore what differences a single electron can make in terms of solvent interactions with solutes. Second, unlike neutral Na_2 in solution, solvated Na_2^+ could be created experimentally. Not only should it be straightforward to prepare $Na_2(THF)_n^+$ clusters in mass-selected supersonic expansions, but Na_2^+ could be prepared in bulk liquid THF at room temperature via pulse radiolysis of solutions containing high concentrations of sodium salts. This should be possible, as it already has been shown that neutral atomic Na species can be created following the radiolysis of Na^+ salts in liquid THF,[9] and these neutral Na species are expected to react in the presence of excess Na^+ to form solution-phase Na_2^+. This will allow us to make a series of predictions about solvent-induced changes in chemical identity that can be directly tested experimentally. Finally, also unlike neutral Na_2, for which the lowest several excited states are bound, the first excited state of the Na_2^+ molecule is dissociative in the gas phase.[10−13] Therefore, this study provides a launching point to understand the effects of solvation on excited states, paving the way for future studies of the photodissociation dynamics of the Na_2^+ species in a variety of solvent environments.

Thus, this paper focuses on understanding solvent effects on the electronic structure of Na_2^+ using MQC MD simulations. We find that, when Na_2^+ is placed inside liquid argon, Pauli repulsion interactions between argon atoms and the Na_2^+ bonding electron result in distortion of the bonding electron density, an effect that induces infrared (IR) activity in what would otherwise be a perfectly symmetric solute with no expected IR absorption. We also see an increase in vibrational frequency and decrease in bond length as confinement of the bonding electron by the surrounding solvent strengthens the Na−Na bond. In contrast, in liquid THF, we find that the sodium dimer cation molecule forms two distinct coordination states due to the dative-bonding interactions between the Na atom cores of Na_2^+ and the THF oxygen sites. Both of these coordination states display opposite trends from Na_2^+ in liquid Ar, with a dramatic lengthening of the bond and decrease in vibrational frequency.

We also have run a series of all-classical simulations of the Na_2^+/THF system, and we find that these hallmark features of the change in chemical identity cannot be correctly described without including quantum mechanics. All-classical simulations can roughly correctly describe the dative-bonding interactions between the solute and the solvent, but when they do, they entirely miss the decrease in vibrational frequency and lengthening of the Na_2^+ bond. If the all-classical simulations are altered to include the known quantum mechanical solution-phase potential of mean force, then the dative bonding is not properly described, since the Pauli repulsion from the quantum electron that determines where dative bonds can form is not explicitly treated. All of the classical simulations emphasize the importance of a quantum treatment of the local specific interactions that can alter chemical identity. When quantum mechanics is considered, even though the dative-bonding interactions are individually weak, the electronic structure of Na_2^+ is modified to such an extent that each of the solvent-coordinated states should be described as unique molecules with properties independent of the original Na_2^+ solute: each of the two stable coordination states has a unique Na−Na bond length, vibrational frequency, spectroscopic signatures, and electronic structure.

To isolate the effects of the weak solvent complexation that changes the chemical identity from more typical solvation, we also show that the THF-coordinated species are stable in the gas phase, highlighting the necessity of treating these species as discrete molecules. The first excited state of the THF-coordinated species is dramatically altered compared to uncoordinated Na_2^+ in the gas phase or in liquid Ar. Gas-phase Na_2^+ has a first excited state with a node perpendicular to the Na−Na bond (a σ^* antibonding orbital), as expected from molecular orbital theory.[14,15] However, the lowest excited state of the coordinated $Na_2(THF)_n^+$ molecules places electron density above and below the bond axis, resembling a π molecular orbital. This means that the electronic properties and excited dynamics of these complexes are entirely different from the uncomplexed molecule: not only is the absorption spectrum of the complexed molecule completely changed from the uncomplexed molecule, but photoexcitation of the complexed molecule will not break the chemical bond in the same way as the uncomplexed molecule. All of the results highlight the importance of including the solvent as part of the chemical identity of the solute when there are local specific interactions that are about the same strength as an H-bond in water.

METHODS

For our MQC MD simulations, we consider the Na_2^+ molecule as two classical Na^+ cores held together by a single quantum-mechanically treated valence bonding electron. Thus, our simulations consisted of hundreds of classical solvent molecules (either Ar or THF), two classical Na^+ cations, and one fully quantum mechanical bonding electron. For the interactions between the classical particles and the quantum mechanical electron, we utilized Phillips−Kleinman (PK) pseudopotentials,[16] modified with polarization potentials to correct for the frozen-core approximation implicit in the PK formalism; these are the same PK pseudopotentials used in our previous work.[1,8,17−19]

https://dx.doi.org/10.1021/acs.jpcb.0c03298
J. Phys. Chem. B 2020, 124, 6603−6616

To understand the importance of including a quantum description of the Na_2^+ bonding electron, we also conducted several comparative all-classical simulations. First, and perhaps most simply, we approximated the Na_2^+ molecule as two Na cores each carrying a half charge with Lennard-Jones (LJ) parameters intermediate between those of a Na^+ and neutral Na. The Na−Na potential was then constructed by fitting the gas-phase Na−Na potential energy curve to a Morse potential. This simulation is referred to as "CL-1". When this simulation failed to reproduce the degree of dative bonding and increase in bond length and lower vibrational frequency of the complexed solute, we also conducted an all-classical simulation where the full charge and Na^+ LJ parameters were restored to the values used in the MQC simulation (with a negative point charge added at the midpoint of the Na−Na bond) and the Na−Na potential altered to match that observed in the MQC simulations. This simulation is referred to as "CL-2". Without the Pauli repulsion from a quantum mechanically treated bonding electron, this simulation predicted that up to three single THF molecules would unphysically bridge the two Na^+ cores. This incorrect dative-bond description led to an incorrect bond length and vibrational frequency for the molecule, despite the use of the "correct" Na−Na interaction. To attempt to do better, we tried a third set of classical simulations utilizing the half-charged sodium cores of the first set but with the "correct" Na−Na potential from the MQC simulations used in the second set. These latter simulations, referred to as "CL-3", showed a marginal improvement in bond length for the complexed molecule but also gave an incorrect description of the dative bonding. Further details of the Na−THF interactions and the Na−Na Morse potentials utilized are provided in the Supporting Information.

All of our simulations of Na_2^+ in THF contained 254 solvent molecules inside a cubic simulation cell with a side length of 32.5 Å. The length of the simulation cell was chosen to match the experimental density of THF at the simulation temperature (0.89 g/mL at ∼298 K). The simulations were performed in the microcanonical ensemble and utilized periodic boundary conditions[20] with the minimum image convention. The classical interactions between the Na^+ cations and the THF solvent molecules were modeled with Lennard-Jones potentials. The THF molecules were treated as rigid, planar five-membered rings following the work of Chandrasekar and Jorgensen.[21] The rigid planarity of the molecules was enforced using the RATTLE algorithm.[22] All interactions in the cells were tapered smoothly to zero at 16 Å over a 2 Å range using a center-of-mass-based switching function developed by Steinhauser.[23] For the quantum mechanical electron in the MQC simulations, the electronic eigenstates were expanded in a basis of 64 × 64 × 64 plane waves that spanned the cubic simulation cell, and the single-electron Hamiltonian was diagonalized at every MD time step using the implicitly restarted Lanczos method as implemented in ARPACK.[24] The MD trajectory was propagated adiabatically on the electronic ground-state surface using the velocity Verlet algorithm[20] with a 4 fs time step. The simulation was subjected to velocity rescaling[20] and then equilibrated for several ps at 298 K before running a 1 ns production trajectory.

MQC simulations of Na_2^+ in Ar were conducted in the same manner as those in THF with the obvious exception of how the solvent was treated. The Na^+−Ar interaction was taken from a fit to the *ab initio* calculations of Reza Ahmadi, Almlöf, and Røeggen.[25] The cubic simulation cell for simulations in Ar had a side length of 43.8 Å and contained 1600 solvent atoms to match the experimental solvent density of Ar at 120 K (1.26 g/mL). For simulations in Ar, the electronic eigenstates were expanded on a basis of 32 × 32 × 32 plane waves spread over a 25 Å box and the MD trajectory was propagated with a 5 fs time step. The Ar simulation state point is well within the liquid region of simulated Ar's phase diagram.[26]

RESULTS AND DISCUSSION

Chelation of Na_2^+ by THF Oxygen Sites Gives Rise to Multiple Stable Coordination States. It is well-known that ethers like THF readily chelate metal cations like Na^+ in solution. For a bare Na^+ in THF, classical simulations predict that the oxygen atoms from six surrounding THFs form dative bonds, with the THF molecules arranged roughly at the corners of an octahedron. In previous work, we performed mixed quantum/classical simulations of neutral Na atoms in THF and found that the solvent pushes the quantum electron density off-center, so that the neutral sodium species in THF solution is best thought of as a Na^+-solvated electron tight contact pair, with the cation end of the contact pair making dative bonds with four THFs on average.[22] Similarly, in our previous studies of Na_2 in THF, we observed that the Na_2 molecule distorts to allow two to four THF oxygen sites to chelate the Na^+ cores on each side of the molecule, for an average coordination of 3.25 THFs per Na^+.[1]

The dative bonds between the THF oxygen sites and sodium core(s) in THF-solvated Na_2^+ are most readily seen in the Na−O pair distribution function, which is shown in Figure 1. For Na_2^+, the pair distribution function shows a large, sharp peak indicative of the Na−THF oxygen site dative-bonding interaction. This peak appears at 2.35 Å, which is the same position that the dative-bonding peak appears in MQC simulations of THF-solvated Na^+−e^- tight-contact pairs[22] and THF-solvated Na_2.[1] Integration of the dative-bonding peak for Na_2^+ reveals an average of 4.88 dative bonds per Na^+ core.

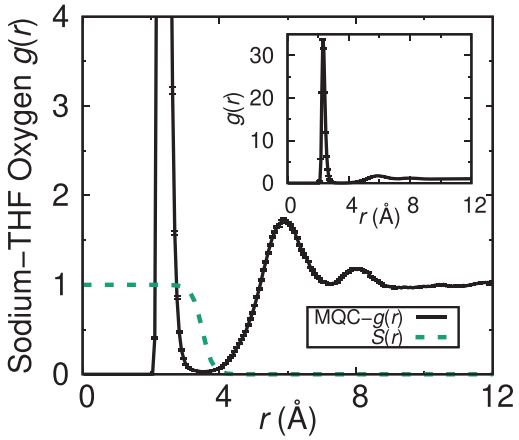

Figure 1. Pair distribution function, $g(r)$, showing the chelation of the Na^+ cores in Na_2^+ by THF oxygen sites, leading to the formation of metal−oxygen dative bonds. The $g(r)$ is averaged over the Na^+−THF oxygen site distances for both Na^+ cores. The smooth weighting function, $S(r)$ (green dashed curve), was used to define the solvent coordination number around each sodium core, as plotted below in Figure 2. The inset shows $g(r)$ on an expanded scale to reveal the full peak height at the ∼2.35 Å dative-bonding distance. The error bars shown represent 95% confidence intervals.

https://dx.doi.org/10.1021/acs.jpcb.0c03298
J. Phys. Chem. B 2020, 124, 6603−6616

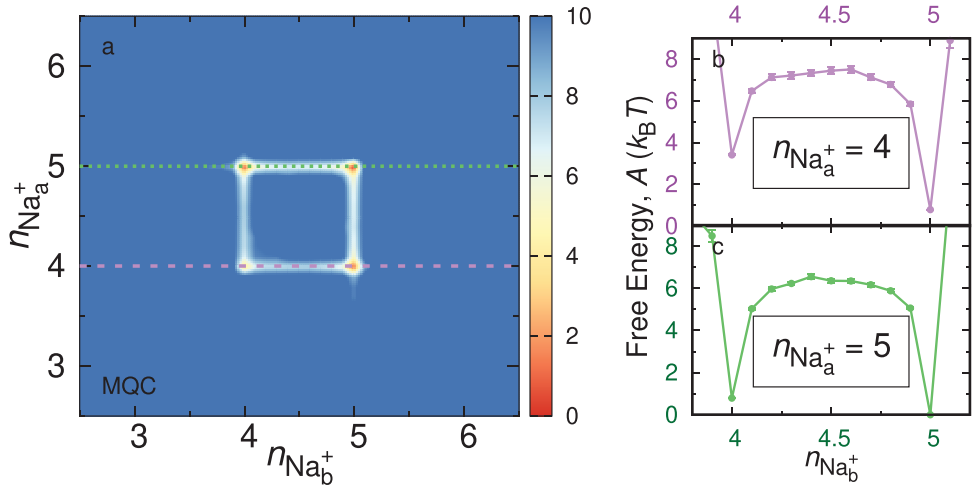

Figure 2. Potential of mean force as a function of the number of Na^+ core−THF oxygen dative bonds on each Na^+ core for MQC simulations; since the Na_a^+ and Na_b^+ cores are identical, the plot is symmetric around the diagonal. The number of dative bonds was determined by summing THF oxygen atoms at each distance weighted by the $S(r)$ function plotted in Figure 1 for each Na^+ core. The energetic minima, shown as red/orange colors in panel a, occur at the integer values of 4 and 5, revealing stable coordination states that are connected by interconversion pathways where a single dative bond is made or broken. Slices along the $n_{Na_b^+}$ coordinate with $n_{Na_a^+} = 4$ (panel b) and $n_{Na_a^+} = 5$ (panel c) show more detail on the heights of the different minima and the barriers between them. A barrier of several k_BT must be surmounted to convert from one stable coordination state to another, indicating that these states are different chemical species. A third coordination state, $Na(THF)_4$−$Na(THF)_4^+$, also can be accessed, but its higher free energy minimum means that it has little Boltzmann weight at equilibrium. The error bars represent 95% confidence intervals.

Table 1. Average Bond Length, Vibrational Frequency, and Instantaneous Dipole Moment for Na_2^+ and Na_2 in the Gas Phase and in Various Solution Environments[a]

system	r_e (Å)	ω_e (cm^{-1})	$\bar{\mu}$ (e-Å)
gas-phase Na_2^+	3.841 ± 0.010	113 ± 29	none
Na_2^+ in argon	3.747 ± 0.007	134 ± 29	0.31 ± 0.10
Na_2^+ in THF^{MQC}	5.237 ± 0.008	42 ± 3	0.9 ± 0.4
Na_2^+ in $THF^{CL\text{-}1}$	3.605 ± 0.003	154 ± 17	none
Na_2^+ in $THF^{CL\text{-}2}$	3.188 ± 0.004	168 ± 21	none
Na_2^+ in $THF^{CL\text{-}3}$	4.067 ± 0.008	82 ± 11	none
$[Na(THF)_4$−$Na(THF)_5^+]_{(THF)}$	4.901 ± 0.013	68 ± 7	1.0 ± 0.4
$[Na(THF)_5$−$Na(THF)]_{(THF)}$	5.65 ± 0.04	56 ± 5	0.8 ± 0.4
$[Na(THF)_4$−$Na(THF)]_{(gas)}$	4.95 ± 0.004	62 ± 6	0.9 ± 0.3
$[Na(THF)_5$−$Na(THF)]_{(gas)}$	5.702 ± 0.006	51 ± 4	0.7 ± 0.3
gas-phase Na_2	3.270 ± 0.004	136 ± 23	none
Na_2 in argon	3.167 ± 0.005	161 ± 48	0.11 ± 0.05
Na_2 in THF^{MQC}	3.617 ± 0.002	112 ± 15	0.6 ± 0.4
$[Na(THF)_3$−$Na(THF)_3]_{(THF)}$	3.472 ± 0.008	119 ± 33	0.4 ± 0.2
$[Na(THF)_2$−$Na(THF)_4]_{(THF)}$	3.66 ± 0.01	108 ± 20	1.2 ± 0.3
$[Na(THF)_3$−$Na(THF)_4]_{(THF)}$	3.692 ± 0.007	113 ± 24	0.7 ± 0.2

[a]The dipole moment's origin is the Na−Na center of mass. The data for Na_2 is taken from ref 1.

To analyze the coordination on each sodium core for Na_2^+ in THF, we utilized a continuous coordination number, which was defined by counting the number of THF oxygen sites that reside within a given distance of the center of each Na^+ core; see the Supporting Information for details. Using this coordinate, whose counting function $S(r)$ is plotted in Figure 1, we calculated the free energy, or potential of mean force (PMF) of the system as a function of n, the number of coordinating solvent molecules on each Na^+ core. These coordinates are labeled Na_a^+ and Na_b^+ in Figure 2.

In Figure 2a, several energetic minima are apparent, all at integer values of coordination, revealing two main stable coordination states: $Na(THF)_4$−$Na(THF)_5^+$ and $Na(THF)_5$−$Na(THF)_5^+$. Slices along the coordination PMF for restricted values of either four ($n_{Na_a^+} = 4$) or five ($n_{Na_a^+} = 5$) THFs coordinated to one of the two sodium cores for the MQC simulation are plotted in Figures 2b and c, respectively. These figures show that the stable energetic coordination minima are separated by energy barriers of many k_BT. The height of the barrier is larger than the direct strength of one of the dative bonds (which is only ∼4 kcal/mol, about the strength of a typical H-bond) because of the solvent reorganization required to change the coordination number. This means that, to break or make a THF−Na core dative bond, i.e., to convert from one coordination state to another, the Na_2^+ molecule must undergo a chemical reaction. We verified that the heights of these barriers are robust for any reasonably defined counting function, $S(r)$.

https://dx.doi.org/10.1021/acs.jpcb.0c03298
J. Phys. Chem. B 2020, 124, 6603−6616

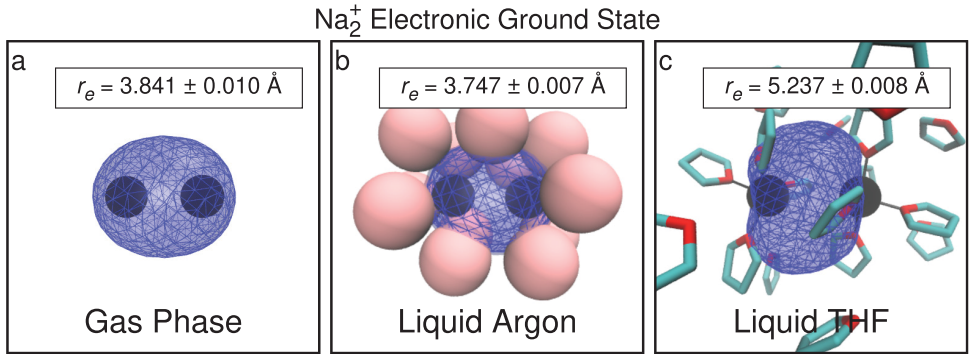

Figure 3. Representative MQC simulation snapshots of Na_2^+ revealing how the presence of solvent molecules deforms the bonding electron density in the condensed phase (b, c) relative to the gas phase (a). The Na^+ cores have been plotted as black spheres scaled to the Na^+ ionic radius, and the valence electron is displayed as a blue wire mesh which contains 90% of the electron density. In panel b, the nearest argon solvent atoms are plotted as pink spheres scaled to argon's van der Waals radius (with a window to allow viewing of the Na_2^+ molecule), while, in panel c, the nearest THF solvent molecules are plotted as turquoise sticks with red oxygen atoms. For THF, the specific configuration shown is in the (4,5) dative-bonding coordination state with four THF molecules forming dative bonds between their oxygen sites and the left-most Na^+ core and five THF molecules forming dative bonds with the right-most Na^+ core. These dative bonds are shown with black lines connecting the THF oxygen sites to the Na^+ core. Note that one dative-bonding THF molecule is partially behind each Na^+ core.

Analysis of the 1 ns MQC Na_2^+ in the THF trajectory revealed reaction times of approximately 32 ± 11 ps for the $Na(THF)_5$–$Na(THF)_5^+$ → $Na(THF)_4$–$Na(THF)_5^+$ reaction and 15 ± 10 ps for the $Na(THF)_4$–$Na(THF)_5^+$ → $Na(THF)_5$–$Na(THF)_5^+$ reaction, times that are consistent with transition state theory, as shown in the Supporting Information. Thus, just as we saw in our previous work of Na_2 in THF, when Na_2^+ is placed in liquid THF, the solvent integrates as part of the chemical identity of the solute.[1] Furthermore, the $Na_2(THF)_n^+$ complexes have higher coordination numbers than the previously observed $Na_2(THF)_n$ complexes, revealing that, even though the single electron of Na_2^+ is more tightly bound in the gas phase, it is easier to push that electron out of the way to expose the cation cores for coordination than it is to distort the two bonding electrons of Na_2. This emphasizes that the properties of the complexed molecule are determined as much by the datively bonded ligands as by the nature of the original gas-phase species.

Table 1 summarizes the average bond length, vibrational frequency, and instantaneous dipole moment for the various THF-solution Na_2^+ coordination states as well as the corresponding values for Na_2 from our previous studies.[1] The origin of the dipole moment was taken to be the Na–Na center of mass; a discussion of the induced dipole moment's orientation with respect to the Na–Na bond axis is provided in the Supporting Information.

The bonding electron of gas-phase Na_2^+ forms a cylindrically symmetric ovoid around the molecule's center of mass, essentially a σ molecular orbital,[14,15] as can be seen in panel a of Figure 3. However, when Na_2^+ is placed in the condensed phase, interactions with solvent molecules deform the bonding electron density. In liquid Ar, Figure 3b, Pauli repulsion interactions with the surrounding cage of argon atoms compress the electron density: the normal exponential decay of the gas-phase wave function out to infinity is curtailed because of Pauli repulsion from the nearby argons, confining the bonding electron via disorder-induced localization. In other words, the bonding electron in liquid Ar is confined both by Coulomb attraction to the Na^+ nuclei and by the irregular, dynamically changing box of the solvent cage. The fact that this confinement produces increased electron density between the nuclei explains the shorter average bond length and the higher vibrational frequency.

Furthermore, the fact that the surrounding solvent cage is asymmetric means that the bonding electron density is not instantaneously centered on the Na–Na bond, creating a fairly large average instantaneous dipole moment of ∼0.3 e-Å, nearly 3 times the value of the instantaneous dipole moment of Na_2 in Ar.[18] This shows that the single bonding electron of Na_2^+ is much more polarizable in Ar than the two bonding electrons of Na_2, likely because the Na_2^+ bond is weaker and thus its electron has a larger surface area with which the Ar solvent atoms can collide. The presence of an instantaneous dipole moment means that, even though Na_2^+ is a nonpolar homonuclear diatomic molecule and Ar is an entirely apolar solvent, the solvated molecule has a changing dipole moment and thus an infrared spectrum. This is an entirely quantum mechanical effect that could not be properly described without a wave function treatment of the bonding electron and its interaction with the surrounding solvent atoms. Thus, even though the structure of the bonding electron for Na_2^+ solvated in Ar bears a general resemblance to the gas-phase Na_2^+, the quantum mechanical interactions with the solvent cause chemically interesting changes to the molecule that differ from what would be expected when considering the molecules in the gas phase alone.

When Na_2^+ is dissolved in liquid THF, in contrast, Figure 3c shows that the system now behaves entirely differently from that in either the gas phase or liquid Ar. The bond length increases significantly and the vibrational frequency decreases, showing that not all liquids have the same general effect on the electronic structure of this solute. As with our previous work on Na_2 in liquid THF,[1] we see that the solvent forces a dramatic distortion of the bonding electron wave function so as to expose the Na^+ cores in the molecular interior. This pushes the bonding electron density away from the ends of the internuclear axis, leading to relatively large instantaneously induced dipole moments as well as a permanent molecular dipole moment for the asymmetrical coordinated state.

Even though this distortion of the bonding electron is energetically unfavorable in the gas phase, in the condensed phase, the distortion is driven by the fact that it allows for better solvation by the surrounding THF molecules in two

https://dx.doi.org/10.1021/acs.jpcb.0c03298
J. Phys. Chem. B 2020, 124, 6603–6616

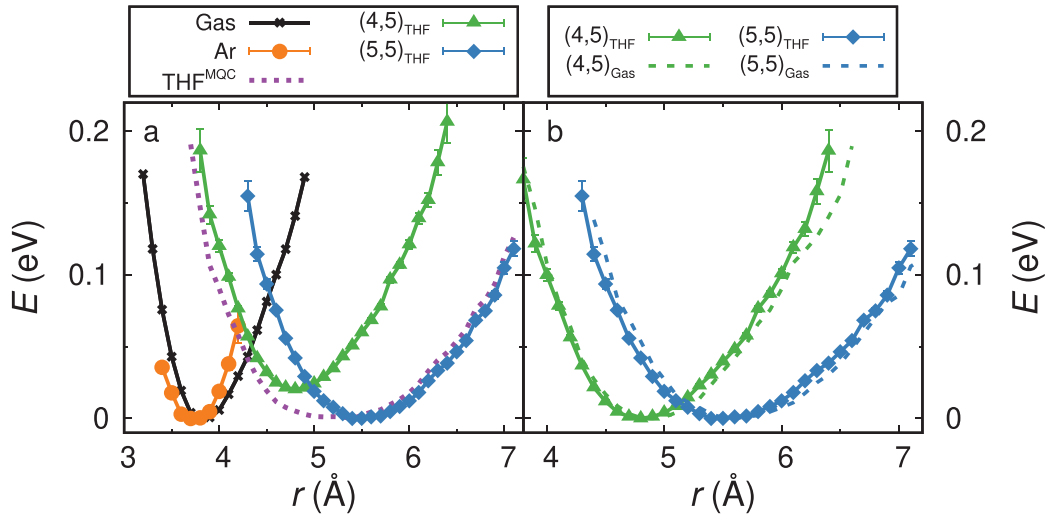

Figure 4. Different local solvent environments lead to different potentials of mean force for the Na_2^+ molecule. In panel a, the gas-phase potential energy surface, as calculated with our MQC model, is plotted in black with the minimum set to zero. The different colored curves show the MQC PMFs in different environments: orange for Na_2^+ in liquid argon and dashed purple for the overall dynamics of Na_2^+ in THF. Notably, the overall PMF in liquid THF is not smooth but shows a small bump near the bottom of the energetic well where the statistics are highest. This is because the Na_2^+ molecule exists in multiple interconverting coordination states in THF; therefore, the full PMF is a Boltzmann-weighted average of the PMFs of the individual coordination states. The individual MQC PMFs for the two stable coordination states are shown in green for $Na(THF)_4$–$Na(THF)_5^+$ and blue for $Na(THF)_5$–$Na(THF)_5^+$, shifted in energy according to their Boltzmann-weighted contributions to the overall PMF of Na_2^+ in THF. Panel b plots a comparison between the MQC $Na_2(THF)_n^+$ coordination states in the gas and condensed phases, with the gas phase plotted as dashed lines and the liquid phase as solid lines; the PMF minimum is set to zero for all four curves for ease of comparison. Clearly, the complexed molecules show only modest changes in their properties upon solvation, similar to dissolving uncomplexed Na_2^+ in liquid Ar.

ways. First, the distortion allows for the creation of dative bonds between the THF oxygen atoms and the cation cores on the molecule; Figure 3c shows a configuration with four THFs datively bonded to one core and five to the other, labeled $Na(THF)_4$–$Na(THF)_5^+$ or simply (4,5). Second, the complexed molecule is asymmetric and has a large dipole and quadrupole moment, providing a handle for the non-datively bonded THFs to use their dipoles to provide extra solvation stabilization. For Na_2, this led to a bond length that was, on average, ~0.35 Å longer than gas-phase Na_2. Without the extra valence electron to help hold the molecule together, Na_2^+ in THF is stretched even further, with an average bond length that is nearly 1.4 Å longer than gas-phase Na_2^+.

The idea that the weakly interacting solvent molecules have become part of the chemical identity of the solute is more than just a semantic definition; it has real implications for the behavior of the Na_2^+ molecule in liquid THF. To illustrate this, Figure 4a compares the potential energy surface (PES) along the Na–Na bond distance of the gas-phase Na_2^+ molecule (black curve) to the PMF along this coordinate for Na_2^+ in liquid Ar (orange curve) and in liquid THF; the purple dashed curve shows the average behavior in THF, and the green and blue curves show the individual PMFs for the two stable coordination states. The average PES of the quantum-treated molecule in THF shows what appears to be unphysical behavior—an imaginary vibrational frequency—in the region near the bottom of the potential well. This behavior can be explained, however, by the fact that quantum Na_2^+ in THF is not a single molecule but instead is made of two distinct chemical species that are in equilibrium with each other: the average PES is simply the Boltzmann-weighted average of the surfaces of the individual species. Each of these species differs only in the number of coordinating solvent molecules, and it is clear from Figure 4a that each of the unique coordination states has its own distinct bond length and vibrational frequency. Clearly, the coordination states must be thought of as separate molecules for the average behavior to be properly understood.

Unlike the case in Ar, where the shorter bond length and higher vibrational frequency of Na_2^+ are readily explained by the solvent confinement of the bonding electron density due to Pauli repulsion, the bond length of the molecule in THF is longer and the vibrational frequency is lower than those in the gas phase. This clearly is related to the dative bonding by the complexed solvent molecules, but the changes in Na_2^+ bond structure in THF also pose an important question: since the molecule has changed chemical identity in THF solution, what is the best gas-phase/condensed-phase comparison? We believe that it makes more sense to compare the condensed-phase behavior to a gas-phase species that includes the THF molecules forming dative bonds to the sodium cores. Indeed, we find that $Na_2(THF)_n^+$ species are stable in the gas phase. This allows us to make a direct comparison between the gas-phase and condensed-phase coordinated species, which is shown in Figure 4b.

We find that, for the complexed species, solvation in the condensed phase produces only a small decrease in the average bond length and a small increase in vibrational frequency; this means that the effects of solvating the datively bonded complex in THF are similar to those that take place when solvating uncomplexed Na_2^+ in liquid Ar. However, the differences observed between the gas- and condensed-phase $Na_2(THF)_n^+$ complexes are on average less than those of Na_2^+ in the gas phase versus Na_2^+ solvated in liquid Ar. For instance, the Na_2^+ bond length is compressed on average by 0.1 Å when the molecule is solvated in argon, but the bonds of the $Na_2(THF)_n^+$ complexes are only compressed by half as much when solvated in THF. This is because the datively bonded

https://dx.doi.org/10.1021/acs.jpcb.0c03298
J. Phys. Chem. B 2020, 124, 6603–6616

THF molecules actually shield the bonding electron from some of the bulk solvent effects, lessening the overall degree of quantum solvation effects on the complexed molecule.

Classical Simulations Fail to Reproduce the Condensed-Phase Bond Dynamics and Chemical Identity of Na_2^+ in THF. Previous work from our group studying Na_2 in liquid Ar found that all-classical simulations failed to capture solvent-induced changes to the Na_2 bonding electrons due to local Pauli repulsion interactions and therefore could not reproduce the important features to the solute's dynamics in the condensed phase.[8] For instance, although the physical confinement of the Na_2 solute by the surrounding cage of Ar solvent atoms led to an increased vibrational frequency in the all-classical simulations, the effect was underestimated by a factor of ∼4, indicating that the solvent-induced quantum effects were a much more important factor in determining the changes to a solute's bond vibrational frequency.[8] Since simulations of a symmetric dimer molecule solvated in an apolar solvent require explicit quantum treatment of the solute's bonding electron to capture the bond dynamics, how well can all-classical simulations hope to capture the complex behavior of a solute in an environment with locally specific solute−solvent interactions? Here, we answer this question by making direct comparisons between MQC simulations where the bonding electron is treated quantum mechanically and a series of simulations in which the entire system is treated classically.

For the first set of all-classical simulations (CL-1), we tried the simplest thing, assuming that the Na−Na interaction is the same as in the gas phase and that the presence of the bonding electron reduced the charge on each Na to +0.5 *e* (with a corresponding slight increase in the Lennard-Jones size of each sodium). When these simulations failed to give a reasonable description of the coordinated molecule, as described below, we then conducted a second set of all-classical simulations (CL-2) where the full charge and Na^+ LJ parameters were restored to the values used in the MQC simulation and a negative point charge was added to the midpoint of the Na−Na bond. The Na−Na potential in CL-2 was also altered to match the PMF observed in the MQC simulations. Figure 5 plots the Na−O pair distribution functions for these two all-classical simulations.

As can be seen in Figure 5, the dative-bonding peak for CL-2 (gray curve) appears at the same location (∼2.35 Å) and with a similar sharpness to that of the MQC simulation of Na_2^+ in THF (black curve). However, the dative-bonding peak for CL-1 is broader and shallower, suggesting that the coordinating THF molecules are held more loosely. This makes sense because each sodium core in CL-1 carries only half a positive charge rather than the full positive charge in the MQC and CL-2 simulations. Furthermore, the dative-bond distance between each $Na^{+0.5}$ core and the oxygen sites of the chelating THFs is larger because the $Na^{+0.5}$ cores are larger to account for the extra half-electron assumed to reside on each. In other words, the simplest all-classical model, CL-1, has no polarizability of the bonding electron; its rigid, fixed electronic geometry is not reflective of the molecule when treated quantum mechanically. All of this indicates that properly representing the interaction of the bare sodium cores with the THF molecules is critical to correctly explaining the dative-bonding environment of this solute.

Although CL-1 does a poorer job than CL-2 of describing the positions of the dative bonds, integration of the dative-bonding peak in the radial distribution function shows that CL-1 actually does a better job of describing the number of dative bonds. CL-1 has an average of 4.46 solvent molecules forming dative bonds with each $Na^{+0.5}$, which is quite similar to the MQC value of 4.88 dative bonds per each Na^+ core, but CL-2 has a significantly higher average coordination around each Na^+ core of 5.93. Clearly, the classical interactions alone are not enough to describe both the position and number of dative bonds formed, emphasizing the importance of having a quantum description of the bonding electron.

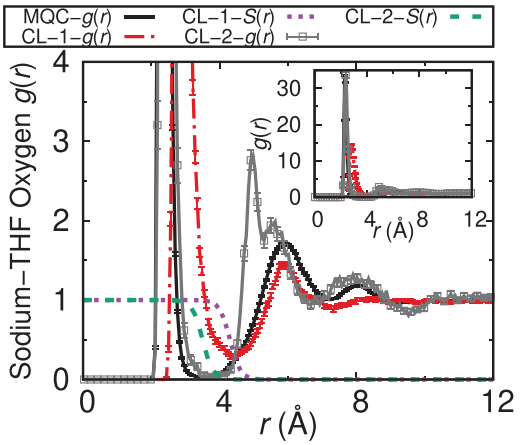

Figure 5. Pair distribution function, $g(r)$, showing the chelation of the sodium cores in Na_2^+ by THF oxygen sites, leading to the formation of metal−oxygen dative bonds for the CL-1 (red curve) and CL-2 (gray curve) simulations. In both sets of simulations, $g(r)$ is averaged over the sodium−THF oxygen site distances for both sodium cores. The smooth weighting functions, $S(r)$ (dashed curves), were used to define the solvent coordination number around each sodium core, as plotted below in Figure 6. The inset shows $g(r)$ on an expanded scale to reveal the full peak height at the dative-bonding distance. The MQC $g(r)$ (black curve) is replotted here for comparison. The smaller sharp peak in the gray CL-2 curve at about 5 Å is from THF molecules that are also datively bonded to the opposite sodium core. The error bars shown represent 95% confidence intervals.

To further explore the differences between the coordination of these two all-classical simulations with the MQC results, Figure 6 shows the PMFs of the systems as a function of the number of coordinating solvent molecules on each sodium core, defined in the same fashion as for the MQC simulation in Figure 2 but using the $S(r)$ counting functions shown in Figure 5. CL-1 captures some of the coordination effects seen in the MQC simulation, as shown in Figure 6a; however, due to the looser Na^+−THF−oxygen site dative bonds, a wider variety of coordination states are accessed. The barriers between coordination states are also lower, so that the system stays in an individual state for less time (about a ps versus a few tens of ps for the MQC simulation, which we show in the Supporting Information is consistent with what is expected from transition state theory). However, the energetic barriers between coordination states, shown in the energy slices in Figure 6b and c, are still sufficiently large that the molecule prefers integer-valued coordination states, even though the looser dative bonds allow the system to more frequently "slip" off of the reaction pathways, as evidenced by the splotchy regions of lower free energy seen in Figure 6a.

As can be seen in Figure 6d, the restoration of the dative-bonding interaction by returning to the use of fully charged Na^+ cores leads to fewer coordination states separated by

https://dx.doi.org/10.1021/acs.jpcb.0c03298
J. Phys. Chem. B 2020, 124, 6603−6616

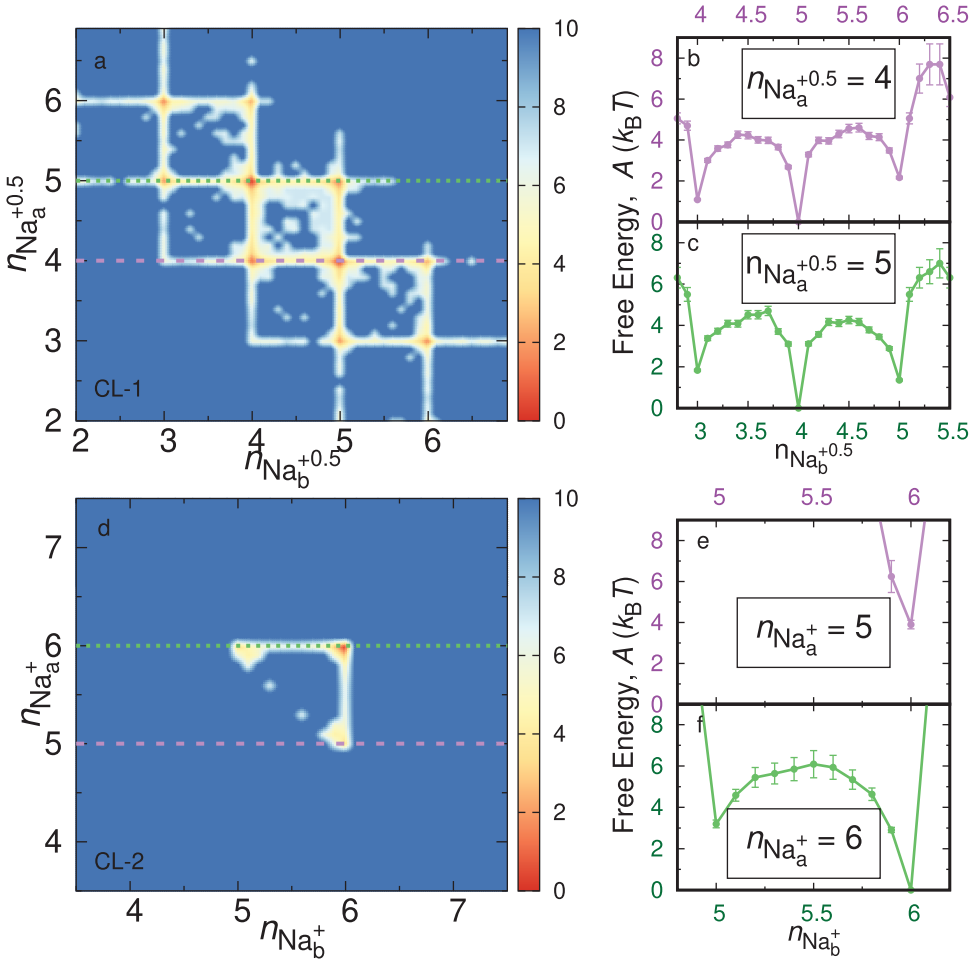

Figure 6. Potential of mean force as a function of the number of sodium core−THF oxygen dative bonds on each sodium core for two all-classical simulations of Na_2^+ in THF, calculated in the same manner as for Figure 2. Panel a reveals that, for CL-1, the system still exhibits energetic minima at integer values of coordination, but the looser classical $Na^{+0.5}$−THF oxygen site dative-bonding interactions allow more coordination states to be accessed, and the individual coordination states are energetically less stable. Panels b and c show slices along the $n_{Na_b^{+0.5}}$ coordinate with $n_{Na_a^{+0.5}} = 4$ in panel b and $n_{Na_a^{+0.5}} = 5$ in panel c. Panel d reveals that CL-2 accesses only two primary coordination states, with five or six datively bonded THFs, which are separated by high energetic barriers. Panels e and f show slices along the $n_{Na_b^{+}}$ coordinate with $n_{Na_a^{+0.5}} = 5$ in panel e and $n_{Na_a^{+0.5}} = 6$ in panel f. The error bars shown represent 95% confidence intervals.

higher energetic barriers for CL-2. This is shown in the slices along $n_{Na_a^{+}} = 5$ and $n_{Na_a^{+}} = 6$, plotted in Figure 6e and f. However, it is important to note that the coordination states accessed have more dative bonds than those accessed by the MQC simulation. Thus, even though these classical simulations can qualitatively capture some of the behavior of this system, it is clear that both of these classical simulations completely miss key features of the quantum mechanical description of dative bonding (and this despite using the "correct" information from the MQC simulations in constructing CL-2).

To obtain a clearer picture of why these all-classical simulations fail, we show representative snapshots from the CL-1 and CL-2 trajectories in Figure 7. Two key differences between the all-classical and MQC simulations are evident from these snapshots. First, the Na−Na bond distance is significantly shorter in both sets of classical simulations, including in CL-2 where the Na−Na potential used had its minimum value at the "correct" MQC bond distance. Second, in both sets of classical simulations, THF molecules are able to "straddle" between the two sodium cores, thus making dative bonds to both sides of the molecule at once. In fact, the only reason that the average number of dative bonds for CL-1 is roughly correct is that the existence of a few multiply dative-bonding THFs that count double make up for the deficit of dative bonding associated with having larger $Na^{+0.5}$ species.

The multiple dative bonding is even more exaggerated for CL-2, where on average three THF molecules are shared between the two sodium cores. Since we never saw multiply bonded THFs in the MQC simulations because Pauli repulsion from the bonding electron prevented THFs from occupying the central region, it is clear that the classical description of these complexes is inadequate. In fact, it is the presence of several multiply dative-bonded THFs that shortens the Na−Na bond length in CL-2 relative to the MQC minimum (~3.188 vs ~5.237 Å, respectively), as collectively the dative-bond interactions in CL-2 are strong enough to pull the molecule to unphysically short bond lengths across the soft MQC Na−Na potential.

To further emphasize this point, Figure 8 plots the PMFs along the Na−Na coordinate for our all-classical simulations of Na_2^+ in THF as well as for the gas-phase Na_2^+ PEC. The red

https://dx.doi.org/10.1021/acs.jpcb.0c03298
J. Phys. Chem. B 2020, 124, 6603−6616

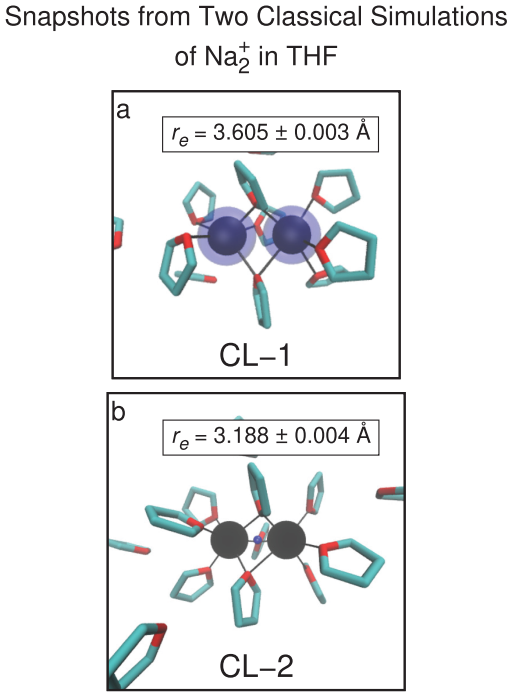

Figure 7. Snapshots from two all-classical simulations of Na_2^+ in THF revealing significantly shorter bond lengths compared to the MQC simulation as well as THF molecules that coordinate both sodium cores at once. Panel a shows a snapshot from CL-1, which uses the gas-phase Na−Na potential and $Na^{+0.5}$ cores; the original Na^+ core radius is drawn as black spheres, and the additional radius used to account for the extra half valence electron on each sodium core is plotted as blue transparent spheres. The nearest THF molecules are shown as turquoise sticks with red oxygen atoms. Panel b shows a snapshot from CL-2, which uses the MQC potential of mean force for the Na−Na interaction, and the same Na^+ cores as the MQC simulation with an extra negative point charge, shown as a small blue sphere, at the Na−Na midpoint. The THF molecules that make bridging dative bonds between the two Na^+ cores pull the Na−Na bond to unphysically short distances, despite the use of the "correct" Na−Na MQC potential.

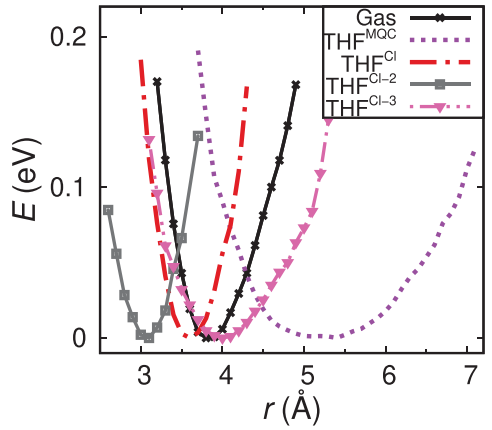

Figure 8. Potentials of mean force for Na_2^+ in THF calculated from three different all-classical simulations: CL-1 (red dot-dashed curve), CL-2 (gray squares), and CL-3 (pink triangles). The gas-phase potential energy surface (black curve) and MQC PMF of Na_2^+ in THF (dotted purple curve) are provided for comparison. Both CL-1 and CL-2 show behavior opposite to the MQC simulation, predicting shorter average bond lengths and higher vibrational frequencies than those of gas-phase Na_2^+. CL-3 qualitatively predicts the correct behavior (longer bond length and lower vibrational frequency) but vastly underestimates these properties compared to the MQC PMF.

dot-dashed curve shows the PMF of CL-1, which clearly has a shorter bond length and higher vibrational frequency than gas-phase Na_2^+. These shifts, which are opposite what is seen in the MQC simulations, take place because of classical confinement of the Na−Na bond by the surrounding solvent. The PMF for CL-2, shown in gray, which was supposed to be an improvement because of its use of the MQC PMF for the Na−Na interaction, is actually unphysical compared to the original CL-1 simulation, with an even shorter average Na−Na bond length. This is because the THFs with multiple dative-bonding interactions dominate the bonding in these simulations: unlike the Pauli repulsion from the bonding electron in the MQC simulations, the negative point charge in the bond center, although repulsive to the THF oxygen sites, is not enough to deter datively bound THF molecules from squeezing the molecule together to allow several THFs to coordinate both sodium cores at the same time.

To see if this deficiency could be easily remedied, we ran a third set of all-classical simulations, CL-3, that utilized the Morse potential from the MQC simulations (same as with CL-2) but the larger $Na^{+0.5}$ cores (that were used in CL-1); the Na−Na PMF for CL-3 is shown as the pink dotted curve in Figure 8, and additional information about these simulations is provided in the Supporting Information. The idea behind constructing CL-3 was that we hoped with weaker dative bonds that it would be harder to push the larger cores together, inhibiting the ability of single THFs to datively coordinate both sodium cores. Indeed, the PMF for CL-3 has improved qualitative behavior, showing an increase in bond length and decrease in vibrational frequency relative to the gas phase, although the size of both shifts is roughly an order of magnitude less than what is seen in the MQC simulation. The dative-bonding environment in CL-3 also is incorrect, appearing similar to that in CL-1 (as might be expected, since the same local interactions are used), as shown in the Supporting Information.

The net conclusion is that classical interactions are insufficient to describe the changes in bonding that take place when there are local specific interactions, such as Na^+−THF dative bonds. It is clear that the quantum mechanical nature of the bonding electron is critical for explaining the bond length, vibrational frequency, and dative-bonding environment and thus also essential to describing the molecule's chemical identity. Even when we used the "exact answer", the PMF from the MQC simulations, we still were unable to reproduce the correct behavior with only classical interactions. Of course, if one were willing to add additional classical interaction sites where the quantum electron sits or include nonlocal or nonpairwise interactions or other adornments, it would undoubtedly be possible to get classical mechanics to reproduce the MQC result, but this could only be done by first knowing the correct answer and then working hard to build interactions to match the known behavior. Clearly, it makes much more sense to start with what is needed for the physics of the problem—a quantum mechanical description of the bonding electron—than to try to build classical models of increasing complexity to achieve the same result.

Discrete $Na_2(THF)_n^+$ Coordination States Can Be Differentiated Experimentally. In addition to having

https://dx.doi.org/10.1021/acs.jpcb.0c03298
J. Phys. Chem. B 2020, 124, 6603−6616

distinct bond lengths and vibrational frequencies, the individual coordinated species in THF also have their own spectroscopic signatures that would allow them to be differentiated by experiment. Figure 9a shows the power

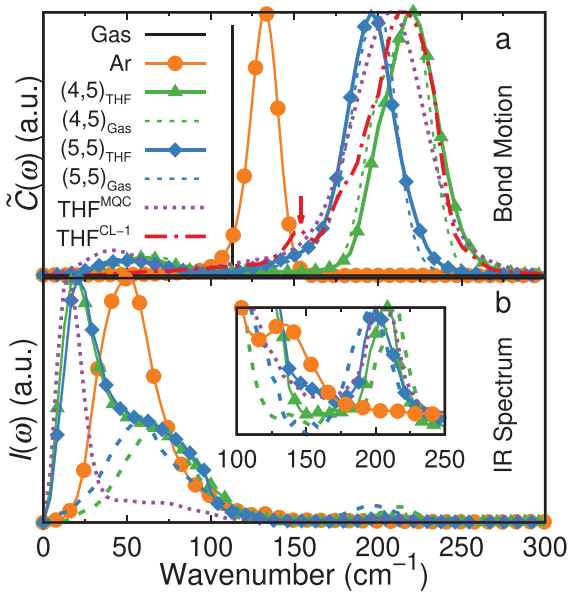

Figure 9. (a) Power spectrum of Na_2^+ calculated from the Fourier transform of the bond velocity autocorrelation function in different environments. The gas-phase vibrational frequency is shown as the black line at 113 cm^{-1}. The orange curve shows the vibrational spectrum of Na_2^+ in liquid Ar. The spectrum is blue-shifted relative to that in the gas phase due to the compression of the bonding electron from Pauli repulsion interactions with the first-shell Ar solvent atoms. However, the spectra in liquid THF (shown as a purple dotted curve for the overall dynamics, green solid curve for $Na(THF)_4$–$Na(THF)_5^+$, blue solid curve for $Na(THF)_5$–$Na(THF)_5^+$, and dashed curves for the $Na_2(THF)_n^+$ complexes in the gas phase) show that the main Na–Na vibration is red-shifted. The second, sharper peak near 200 cm^{-1} corresponds to the vibration of the Na^+–THF oxygen site dative bonds. The all-classical spectrum of CL-1, shown as the dashed red curve, displays a broad dative-bonding peak as well as a small feature at ~150 cm^{-1} (indicated by the red arrow) corresponding to the Na–Na vibrational frequency. (b) Infrared spectrum of Na_2^+ calculated as the Fourier transform of the dipole moment autocorrelation function. Although Na_2^+ has no IR spectrum in the gas phase, all of the condensed-phase environments show strong IR absorption. The largest peaks (at ~50 cm^{-1} in liquid Ar and ~20 cm^{-1} in liquid THF) are due to intermolecular rattling motions in the solvent cage, but specific features from the Na_2^+ vibrational motion are also apparent (~130 cm^{-1} for the Na_2^+ vibration in Ar, ~55 cm^{-1} for Na_2^+ in THF) as well as the ~200 cm^{-1} dative-bond stretches in THF).

spectrum (Fourier transform of the Na–Na bond velocity autocorrelation function) of Na_2^+ in different environments. In liquid argon (orange curve), a single peak is evident, corresponding to a molecular vibration that is blue-shifted from that in the gas phase. However, for the power spectrum of Na_2^+ in THF (plotted as the purple dashed curve, with the green curve for the $Na(THF)_4$–$Na(THF)_5^+$ state and the blue curve for the $Na(THF)_5$–$Na(THF)_5^+$ state), there are two significant peaks for each coordination state: a large, sharp peak at about 200 cm^{-1} and a shallower, broader peak at about 55 cm^{-1}. The shallower, lower frequency peak corresponds to the Na–Na vibrational frequency: this frequency is much lower than that in the gas phase both because of the weaker bond and increased bond length and because the movement of the Na atoms also requires carrying along the heavy datively bonded THF molecules. The location of this peak only marginally shifts when the $Na_2(THF)_n^+$ complexes are taken out of solution (plotted as the dashed green and blue curves), indicating that it is the datively bonded THF molecules that most strongly modulate this motion, with only minor effects from the non-datively bonded solvent molecules.

The second, sharper and higher-frequency peak observed in the power spectrum for the coordinated species in THF corresponds to the dative-bond stretch between the Na cation cores and the complexed THF oxygen atoms. The complexes with different numbers of coordinating THFs have different vibrational frequencies for this dative-bond stretching motion: less-coordinated sodium cation cores hold onto their dative-bonding solvent molecules more tightly, leading to a higher frequency vibration, while more-coordinated cores hold their dative-bonded THFs more loosely, leading to a lower frequency vibration. These dative-bond vibrational peaks appear at the same ~200 cm^{-1} location as previously observed for Na_2 in liquid THF,[1] indicating that this interaction is not strongly influenced by the number of bonding electrons present in the molecule. It is therefore not surprising that the all-classical simulation of Na_2 in THF correctly predicts the location of this peak, albeit broader than the MQC predictions due to the greater variety of coordination states accessed in the all-classical simulation, which leads to more dative-bonding environments averaged into the dative-bond vibrations. However, the CL-1 simulation completely misses the correct Na–Na vibrational frequency, instead predicting it to be even further blue-shifted relative to the gas phase than Na_2^+ in liquid Ar, as indicated by the red arrow in Figure 9a.

The different power spectra strongly suggest that the infrared (IR) spectrum could be used to experimentally investigate the bonding of the Na_2^+ species in different solvent environments. Thus, in Figure 9b, we show the IR spectra of Na_2^+ in each of the various environments, calculated as the Fourier transform of the dipole autocorrelation function. Although the Na_2^+ molecule is not IR active in the gas phase, the fact that Pauli repulsion from the surrounding solvent atoms/molecules pushes the bonding electron off center means that an instantaneous dipole moment is induced. In all solvent environments, this fluctuating dipole gives rise to a large IR absorption peak appearing at low wavenumbers, which corresponds to the dynamics of the solvent cage surrounding the molecule: essentially, this is the frequency of collisions in liquid Ar or the frequency of noncomplexed THF molecular rotations that push on the Na_2^+ bonding electron to induce a net dipole. The calculated IR spectra also show a peak corresponding to the vibrational frequency of the Na_2^+ molecule. This peak is weak in liquid Ar, as the Na–Na stretching motion affects the molecular dipole only indirectly because this motion helps modulate interactions with the surrounding solvent cage that breaks the molecular symmetry. The peak is stronger in liquid THF, as the complexed molecule has a permanent dipole induced by the datively bonded solvents. The IR spectra for the gas-phase $Na_2(THF)_n^+$ complexes lack the large peaks from intermolecular rattling but still show the broad peak for the Na–Na stretching motion. For the THF–complexed molecules, both in and out of solution, the dative-bonding vibrational frequency is also observed in the IR as the Na–THF–oxygen stretch also

https://dx.doi.org/10.1021/acs.jpcb.0c03298
J. Phys. Chem. B 2020, 124, 6603–6616

modulates the dipole of the complex. These observed IR features show that IR spectroscopy would provide a direct handle on the solvent-induced changes in chemical identity.

Finally, we can also simulate the UV−visible absorption spectra for Na_2^+ in different environments, as shown in Figure 10. For Na_2^+ in liquid Ar, the absorption spectrum strongly

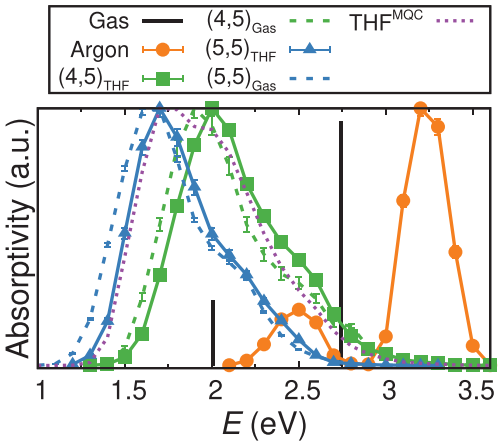

Figure 10. Electronic absorption spectrum of Na_2^+ in various environments revealing the dramatic change in electronic structure in THF including distinct spectral signatures for the different coordination states. The gas-phase absorbance is plotted as vertical black lines whose height represents their relative oscillator strengths. In liquid Ar (orange curve), the Na_2^+ absorption spectrum is blue-shifted and broadened relative to that in the gas phase, reflecting confinement of the bonding electron and the fluctuations of the surrounding solvent. In liquid THF (purple dashed curve), however, the shape of the spectrum is red-shifted and clearly different from that in the gas phase or in liquid Ar. This shows that the electronic structure of THF-complexed Na_2^+ is entirely altered from that in the gas phase, and the spectrum of the individual underlying coordination states is shown as the blue and green solid curves (the corresponding spectra of the complexes in the gas phase are shown as the blue and green dashed curves). The error bars shown represent 95% confidence intervals.

resembles that in the gas phase but with the electronic transitions blue-shifted and broadened. The blue-shift results directly from the compression of the bonding electron by the caging solvent: the spectrum is now that of a molecule in a box rather than just a molecule, and the confinement in the "box" of the solvent cage raises the energy of the larger excited state (see below) more than the ground state, blue-shifting the electronic transitions. In liquid THF, on the other hand, the absorption spectra of the different coordination states of the molecule have an entirely different, red-shifted structure. This is not surprising, as the molecular identity is entirely different. The red shift observed here for Na_2^+ in THF relative to gas-phase Na_2^+ is even larger than the one previously observed for Na_2, indicating that the electronic changes to the single electron are even greater than those for the two electrons of Na_2. Since the change in electronic structure depends on the datively bonded THFs, the spectra of the two different underlying complexes are also different, with the $Na(THF)_4$−$Na(THF)_5^+$ species absorbing to the blue of the $Na(THF)_5$−$Na(THF)_5^+$ species. Each $Na_2(THF)_n^+$ complex displays the expected blue shift relative to its own unique complexed gas-phase counterparts (plotted as the dashed curves in Figure 10) due to solvent confinement of the bonding electron. Clearly, the two different complexed molecules have distinct electronic absorption spectra as well as distinct IR spectra.

The fact that the different complexed species in liquid THF have different electronic absorption spectra means that the overall absorption spectrum for Na_2^+ in THF is inhomogeneously broadened. This means that it should be possible to experimentally distinguish the two species by transient spectroscopy. This is because one could selectively excite only one of two predominant coordination species and then watch the effect on the absorption spectrum as the two re-equilibrate, a classic transient hole-burning experiment.

We have simulated this transient hole-burning experiment, shown in Figure 11, to demonstrate precisely how these discrete coordination states could be probed experimentally. To do this, we took our equilibrium trajectory for the Na_2^+ molecule in THF and calculated the spectrum the molecule would have had following times when the energy gap was resonant on the red edge of the absorption band: in other words, following selective excitation of the $Na(THF)_5$−$Na(THF)_5^+$ species with a pump of approximately 1.7 eV (Figure 11a). The results show that the bleached spectrum at early times resembles that of the solvated $Na(THF)_5$−$Na(THF)_5^+$ species. However, over the approximately 30 ps coordination-state interconversion time, the bleached spectrum undergoes spectral diffusion and broadens until it lies within the error of the calculated average spectrum of Na_2^+ in THF. Similarly, when a pump wavelength of approximately 2.0 eV is used, we see that $Na(THF)_4$−$Na(THF)_5^+$ is selectively bleached (Figure 11b). With a faster interconversion time of ∼15 ps, reflecting the fact that this coordination state is less stable than the $Na(THF)_5$−$Na(THF)_5^+$ state, the spectrum broadens until it again is within the error of the average spectrum. This suggest that transient hole-burning experiments could be used to distinguish the discrete coordinated states of $Na_2(THF)_n^+$ and measure their interconversion time, either in mass-selected clusters in a supersonic expansion or in the bulk room-temperature liquid.

Distortion of the Na_2^+ First Excited State in THF. In the gas phase, the first excited state of the Na_2^+ molecule is dissociative. This means that this solute offers a unique chance to study condensed-phase photodissociation dynamics and how those dynamics change when the chemical identity of the molecule is altered by interactions with the solvent. Indeed, as shown in Figure 12a, in the gas-phase first excited state, the bonding electron density is equally distributed between the two sodium cores, exactly as expected for an antibonding σ^* orbital in molecular orbital theory:[14,15] the excited electron has a node that sits perpendicular to the bond axis. In liquid Ar (Figure 12b), the same basic electronic structure is observed, with some perturbations due to the surrounding cage of Ar atoms; one can see that the reason the electronic absorption spectrum in liquid Ar is blue-shifted relative to the gas phase is that the excited-state wave function is more strongly confined in the liquid than the ground-state wave function.

In stark contrast, Figure 12c shows that, when there are local specific interactions between THF molecules and Na_2^+, as in the (4,5) coordination state, the electronic structure of the excited state is completely altered: the bonding density is confined between the two nuclei rather than being pushed outside the nuclei, and there is a node that is parallel to the bond axis rather than normal to it. Thus, the Na_2^+ THF-coordinated species have a lowest-energy excited state that better resembles a molecular π orbital than a σ^* orbital

https://dx.doi.org/10.1021/acs.jpcb.0c03298
J. Phys. Chem. B 2020, 124, 6603−6616

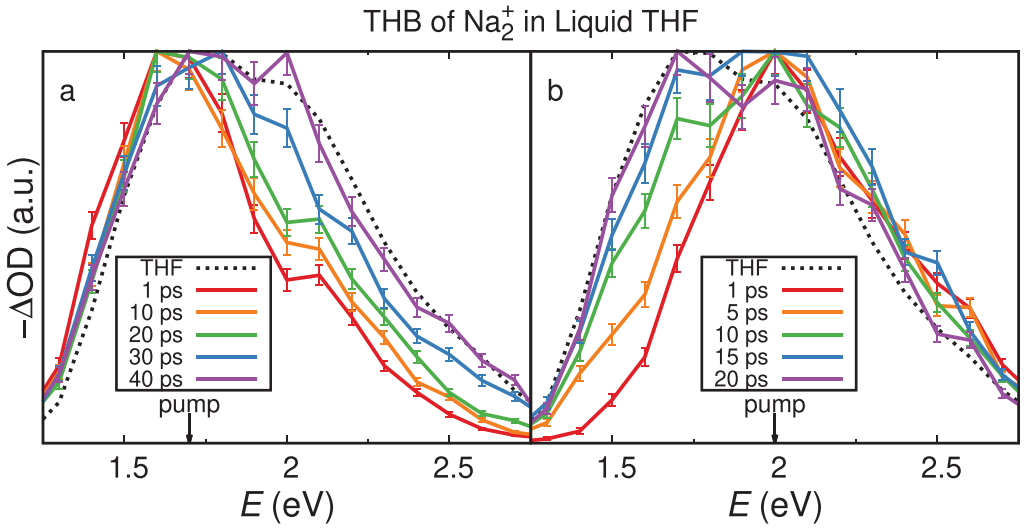

Figure 11. Simulated transient hole-burning showing that the underlying coordination states could be readily distinguished experimentally because the underlying spectrum is inhomogeneously broadened. Panel a shows that, following excitation at approximately 1.7 eV, a spectral position where $Na(THF)_5$–$Na(THF)_5^+$ absorbs strongly but $Na(THF)_4$–$Na(THF)_5^+$ does not, there is a selective bleach of the $Na(THF)_5$–$Na(THF)_5^+$ contribution to the total spectrum. The interconversion between the complexed species that takes place on a tens-of-ps time scale leads to spectral diffusion, so that eventually the entire band is bleached. Panel b shows that excitation at approximately 2.0 eV similarly selectively bleaches only the $Na(THF)_4$–$Na(THF)_5^+$ species at early times; spectral diffusion to the full spectrum takes place more quickly, as this species is less stable and has a lower Boltzmann weight in the equilibrium. These results show that transient hole-burning could probe the discrete coordination states present in a bulk solution of Na_2^+ in THF. The error bars shown represent 95% confidence intervals.

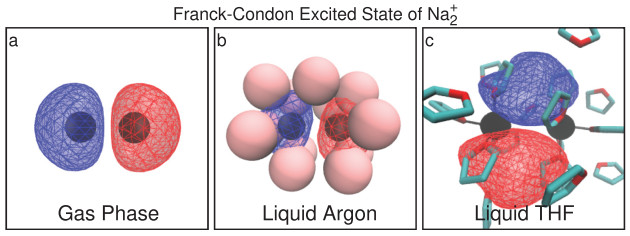

Figure 12. Snapshots of the lowest electronic excited state of Na_2^+ in different environments revealing an entirely different electronic structure in THF than in the gas phase or liquid Ar. In the gas phase (a), the wave function of the first excited state (the red and blue colors denote opposite phases) distributes equally between each Na^+ core with a node perpendicular to the bond axis located at the center of the molecule, much like the σ^* antibonding orbital expected from molecular orbital theory. In liquid Ar (panel b), the wave function distributes in a similar manner, with some perturbations and additional confinement due to the surrounding cage of Ar atoms. However, in THF (panel c), the molecule's first excited state has an entirely different structure: the wave function is confined to reside between the nuclei rather than outside them, with a node along the internuclear axis, similar to a molecular π bond. This suggests that, although the Na_2^+ molecule photodissociates in the first excited state in the gas phase and liquid Ar, the dynamics following photoexcitation of Na_2^+ in THF will follow an entirely different pathway.

(although we show in the Supporting Information that the third excited state has σ^* character). This behavior holds true for the Na_2^+ coordinated states both in and out of the condensed phase. This means that photoexcitation of a THF-complexed Na_2^+ molecule would not lead to immediate photodissociation: the bond may weaken upon Franck–Condon excitation, but there is no reason to expect a strong dissociative force along the Na–Na bond distance coordinate, as would take place in the gas phase or liquid Ar. Moreover, the excited-state wave function also appears to interact with the datively bonded THFs in a different way than the ground state, so that photoexcitation may be coupled with a possible change in the chemical identity of the molecule. We will explore the excited-state molecular dynamics of Na_2^+ in all of these different environments in a future investigation.

The dramatically different excited-state electronic structure for what is nominally the same Na_2^+ molecule is what give rises to the differences in the UV–vis spectra shown above in Figure 10. The change in electronic structure with solution environment changes not only the excited-state wave function in the Franck–Condon region but also the entire equilibrium potential energy surface of the molecule. Figure 13 shows the potential energy curves (PECs) of the ground and first excited states of the gas-phase Na_2^+ molecule and of the gas-

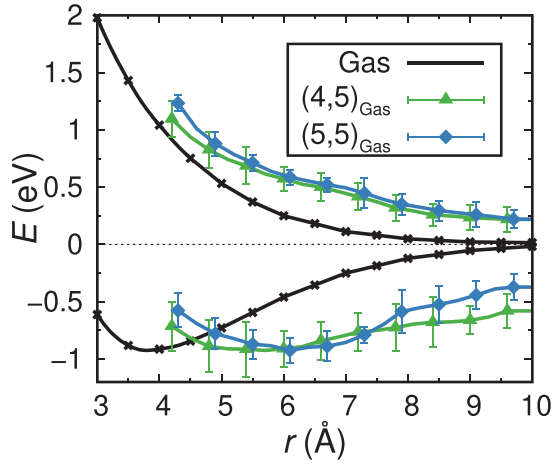

Figure 13. Potential energy curves (PECs) of the ground and first excited states of Na_2^+ and the $Na_2(THF)_n^+$ coordinated structures in the gas phase. Clearly, the dynamics upon photoexcitation would be very different for the Na_2^+ in the gas phase and when solvated in liquid THF.

https://dx.doi.org/10.1021/acs.jpcb.0c03298
J. Phys. Chem. B 2020, 124, 6603–6616

phase coordinated $Na(THF)_4$–$Na(THF)_5^+$ and $Na(THF)_5$–$Na(THF)_5^+$ molecules; the latter curves are calculated as room-temperature equilibrium averages along the ground-state PMFs by holding the Na–Na bond distance at different lengths and allowing the coordinated solvent molecules to fluctuate. The figure makes it clear that, when Na_2^+ is complexed by THF, the excited-state dynamics will follow an entirely different pathway than the bare molecule in the gas phase because of the large changes in the excited-state wave function induced by the presence of the datively bonded solvents. It is important to note that is clearly a quantum mechanical effect. This also opens the interesting question as to whether or not the actual dynamics will follow the PECs shown in Figure 13, which are linear response predictions, as the solvent motions (including the datively bonded THFs) might be entirely different on the ground and first excited states. Clearly, the ways in which solvent molecules interact with the electronic structure of solutes are not negligible, and we must go beyond a "gas-phase potential surfaces transfer directly to the liquid" picture if we are to understand chemical bond dynamics in condensed phases.

CONCLUSIONS

In summary, comparative all-classical and MQC simulations of Na_2^+ in liquid Ar and liquid THF reveal that treating the solute's bonding electron explicitly quantum mechanically is necessary to understand the condensed-phase dynamics of this or indeed any solute. Even for simulations in apolar Ar, neglect of quantum effects of the solvent on the bonding electron density misses important features, such as the fluctuating dipole moment and thus the IR activity of Na_2^+ induced by Pauli repulsion forces in the condensed phase. For Na_2^+ in THF, all-classical simulations not only miss these features but also predict changes in the bond length and vibrational frequency of the molecule that are completely opposite to the correct behavior. Even with prior knowledge of the MQC results, it is not trivial to describe solvent effects on the bond dynamics and chemical identity of the solute using classical mechanics.

As we saw previously in studies of Na_2 in THF,[1] Na_2^+ in THF exists in several stable, interconverting coordination states that behave as discrete molecules with their own bond dynamics and spectral signatures. All of the changes in chemical identity we noted in our previous work[1] are magnified when one of the bonding electrons of the molecule is removed: the solvent has an easier time altering the electronic structure of the sodium dimer cation than the neutral sodium dimer simply because it is easier to create dative bonds with the sodium cation cores when there's only one electron to push out of the way. For the sodium dimer cation, we also have shown that these coordinated states are stable in the gas phase and thus should be the "true" gas-phase reference molecules for understanding the $Na_2(THF)_n^+$ coordinated species in the condensed phase, even though the strength of an individual dative bond is only ~4 kcal/mol. Perhaps more importantly, we have predicted that these unique chemical species not only have distinct bond lengths and IR spectra but also that they can be distinguished experimentally through transient hole-burning experiments by bleaching one of the primary species and watching the spectral diffusion that interconverts the stable coordination states.

Finally, our MQC studies of Na_2^+ in THF also suggest that the electronic structure of the solute is dramatically altered by the local solvent environment, as shown by the completely different shape of the excited-state wave function and the correspondingly altered UV–vis spectra of the $Na_2(THF)_n^+$ complexes compared to the gas phase. The coordination states also have potential energy surfaces that are qualitatively different from those of the gas-phase molecule, which suggests that the basic chemical identity of the solute, including its reactivity such as the breaking of the bond by photodissociation, will be entirely different for the $Na_2(THF)_n^+$ coordinated structures than for Na_2^+ in other environments.

ASSOCIATED CONTENT

Supporting Information

The Supporting Information is available free of charge at https://pubs.acs.org/doi/10.1021/acs.jpcb.0c03298.

Further simulation and calculation details (PDF)

AUTHOR INFORMATION

Corresponding Author

Benjamin J. Schwartz – *Department of Chemistry & Biochemistry, University of California, Los Angeles, Los Angeles, California 90095-1569, United States;* orcid.org/0000-0003-3257-9152; Phone: (310) 206-4113; Email: schwartz@chem.ucla.edu

Author

Devon R. Widmer – *Department of Chemistry & Biochemistry, University of California, Los Angeles, Los Angeles, California 90095-1569, United States*

Complete contact information is available at: https://pubs.acs.org/10.1021/acs.jpcb.0c03298

Notes

The authors declare no competing financial interest.

ACKNOWLEDGMENTS

The authors thank the US Department of Energy Condensed Phase and Interfacial Molecular Science program (Grant 0000228903) for supporting this work. The authors also thank the Institute for Digital Research and Education (IDRE) at UCLA for use of the hoffman2 computing cluster.

REFERENCES

(1) Widmer, D. R.; Schwartz, B. J. Solvents can control solute molecular identity. *Nat. Chem.* **2018**, *10*, 910–916.

(2) Young, R. M.; Neumark, D. M. Dynamics of solvated electrons in clusters. *Chem. Rev.* **2012**, *112*, 5553–5577.

(3) Blandamer, M. J.; Fox, M. F. Theory and applications of charge-transfer-to-solvent spectra. *Chem. Rev.* **1970**, *70*, 59–93.

(4) Marcus, R. A. On the theory of oxidation-reduction reactions involving electron transfer. *J. Chem. Phys.* **1956**, *24*, 966–978.

(5) Marcus, R. A.; Sutin, N. Electron transfers in chemistry and biology. *Biochim. Biophys. Acta, Rev. Bioenerg.* **1985**, *811*, 265–322.

(6) Barthel, E. R.; Martini, I. B.; Schwartz, B. J. How does the solvent control electron transfer? Experimental and theoretical studies of the simplest charge transfer reaction. *J. Phys. Chem. B* **2001**, *105*, 12230–12241.

(7) Harris, A. L.; Brown, J. K.; Harris, C. B. The nature of simple photodissociation reactions in liquids on ultrafast time scales. *Annu. Rev. Phys. Chem.* **1988**, *39*, 341–356.

(8) Glover, W. J.; Larsen, R. E.; Schwartz, B. J. How does a solvent affect chemical bonds? Mixed quantum/classical simulations with a full CI treatment of the bonding electrons. *J. Phys. Chem. Lett.* **2010**, *1*, 165–169.

(9) Bockrath, B.; Dorfman, L. M. Pulse radiolysis studies. XXII. Spectrum and kinetics of sodium cation-electron pair in tetrahydrofuran solutions. *J. Phys. Chem.* **1973**, *77*, 1002−1006.
(10) Zhang, Q.; Hepburn, J. W.; Shapiro, M. Observation of above-threshold dissociation of Na_2^+ in intense laser fields. *Phys. Rev. A* **2008**, *78*, 021403.
(11) Fayeton, J. A.; Barat, M.; Brenot, J. C.; Dunet, H.; Picard, Y. J.; Saalmann, U.; Schmidt, R. Detailed experimental and theoretical study of collision-induced dissociation of Na_2^+ ions on He and H_2 target at keV energies. *Phys. Rev. A: At., Mol., Opt. Phys.* **1998**, *57*, 1058−1068.
(12) Brenot, J. C.; Dunet, H.; Fayeton, J. A.; Barat, M.; Winter, M. Analysis of collision induced dissociation of Na_2^+ molecular ions. *Phys. Rev. Lett.* **1996**, *77*, 1246−1249.
(13) Henriet, A.; Masnou-Seuws, F. Model potential calculations for the ground, excited and Rydberg $^2\Sigma$ states of Li_{2+}, Na_2^+ and K_2^+: Core polarization effects. *Chem. Phys. Lett.* **1983**, *101*, 535−540.
(14) Lennard-Jones, J. E. The electronic structure of some diatomic molecules. *Trans. Faraday Soc.* **1929**, *25*, 668−686.
(15) Coulson, C. A. Representation of simple molecules by molecular orbitals. *Q. Rev., Chem. Soc.* **1947**, *1*, 144−178.
(16) Phillips, J. C.; Kleinman, L. New method for calculating wave functions in crystals and molecules. *Phys. Rev.* **1959**, *116*, 287−294.
(17) Smallwood, C. J.; Larsen, R. E.; Glover, W. G.; Schwartz, B. J. A computationally efficient exact pseudopotential method. I. Analytic reformulation of the Philips-Kleinman theory. *J. Chem. Phys.* **2006**, *125*, 074102.
(18) Smallwood, C. J.; Mejia, C. N.; Glover, W. G.; Larsen, R. E.; Schwartz, B. J. A computationally efficient exact pseudopotential method. 2. Application to the molecular pseudopotential of an excess electron interacting with tetrahydrofuran (THF). *J. Chem. Phys.* **2006**, *125*, 074103.
(19) Glover, W. J.; Larsen, R. E.; Schwartz, B. J. The roles of electronic exchange and correlation in charge-transfer-to-solvent dynamics: Many-electron nonadiabatic mixed quantum/classical simulations of photoexcited sodium anions in the condensed phase. *J. Chem. Phys.* **2008**, *129*, 164505.
(20) Allen, M. P.; Tildesley, D. J. *Computer Simulation of Liquids*; Oxford University Press: London, 1992.
(21) Chandrasekhar, J.; Jorgensen, W. L. The nature of dilute-solutions of sodium-ion in water, methanol, and tetrahydrofuran. *J. Chem. Phys.* **1982**, *77*, 5080−5089.
(22) Glover, W. J.; Larsen, R. E.; Schwartz, B. J. Nature of sodium atoms/(Na+-e-) contact pairs in liquid tetrahydrofuran. *J. Phys. Chem. B* **2010**, *114*, 11535−115439.
(23) Steinhauser, O. Reaction field simulation of water. *Mol. Phys.* **1982**, *45*, 335−348.
(24) Allen, M. P.; Tildesley, D. J. *ARPACK Users' Guide*; SIAM: Philadelphia, 1998.
(25) Reza Ahmadi, G.; Almlöf, J.; Røeggen, I. The interaction potential for the $X^1\Sigma^+$ state of $ArNa^+$, $NeNa^+$ and $HeNa^+$. *Chem. Phys.* **1995**, *199*, 33−52.
(26) Smit, B. Phase-diagrams of Lennard-Jones fluids. *J. Chem. Phys.* **1992**, *96*, 8639−8640.

https://dx.doi.org/10.1021/acs.jpcb.0c03298
J. Phys. Chem. B 2020, 124, 6603−6616